文章编号: 1007 - 4252(2011)04 - 0366 - 11

Optical Properties of Poly(N-Phenylmaleimide)-b-Poly(4-Vinylpyridine)-CdS Nanocomposites

Dong Yan-mao[1,2], Lu Jian-mei[1], Lei Hu[1], Ji Shun-jun[1]
(1. Key Laboratory of Organic Chemistry of Jiangsu Province, College of chemistry, chemical engineering and materials science, Soochow University, Suzhou, 215123; 2. School of Chemistry and Bioengineering, Suzhou University of Science and Technology, Suzhou, 215009)

Abstract: The amphipathic poly(N-phenylmaleimide)-b-poly(4-vinylpyridine)-Cd^{2+} (PNPV-Cd^{2+}) complex has been synthesized by reversible addition fragmentation chain transfer (RAFT) polymerization. The 4VP groups acted as the coordination sites for cadmium ion aggregations and nanosized CdS particles were successfully grown in situ at these sites with the release of S^{2-} ions from thioacetamide. The CdS content and size in poly(N-phenylmaleimide)-b-poly(4-vinylpyridine)-CdS (PNPV-CdS) nanocomposites were controlled by the polymerization time. The optical properties of the prepared PNPV-CdS nanocomposites were characterized by linear absorption and photoluminescence (PL) spectra. The PL properties of the nanocomposites are controllable by RAFT method. Z-scan measurement was also employed to investigate the third-order nonlinear optical (NLO) properties at a wavelength of 532 nm. The nonlinear optical response of PNPV-CdS is much stronger than that of CdS and PNPV. This nanocomposite has potential applications in all-optical switches in optical information processing.

Keywords: RAFT; N-phenylmaleimide; nanocomposite; photoluminescence; nonlinear optical

聚(N-苯基马来酰亚胺)-b-聚(4-乙烯基吡啶)-CdS 纳米复合物的光学性质

董延茂[1,2],路建美[1],胡磊[1],纪顺俊[1]
(1. 江苏省有机化学重点实验室,苏州大学材化部,江苏苏州,215123;
2. 苏州科技学院化学与生物工程学院,江苏苏州,215009)

摘要: 用可逆加成锻炼链转移(RAFT)聚合方法合成了两亲性聚(N-苯基马来酰亚胺)-b-聚(4-乙烯基吡啶)-Cd^{2+}(PNPV-Cd^{2+})高分子配合物。Cd^{2+}离子与 4VP 基团配位并与硫代乙酰胺分解产生的 S2-离子原位生成 CdS 纳米粒子。聚(N-苯基马来酰亚胺)-b-聚(4-乙烯基吡啶)-CdS(PNPV-CdS)中 CdS 的含量可通过 RAFT 聚合时间进行调控。用紫外吸收和荧光光谱(PL)测试了 PNPV-CdS 的光学性质。PNPV-CdS 的 PL 性质可通过 RAFT 方法进行控制。用 Z-扫描的方法在 532 nm

Received Date: 2010 - 09 - 12; Modified Date: 2011 - 03 - 23

The first author: Dong Yan - mao (1970 -), associate professor, Ph. D, The main research direction is the photoelectric and environmental functional materials. E - mail: dongyanmao@163.com, tel. /fax: +8651265882875.
Corresponding author: Lu Jian - mei; Address: Renai road, Suzhou industry park, Suzhou, China. Fax: +8651265882875; Tel: +8651265882875; E - mail: lujm@suda.edu.cn.

波长下研究了 PNPV-CdS **的三阶非线性光学(** NLO**) 性质。** PNPV-CdS **的** NLO **响应分别强于** CdS **和** PNPV。**这种纳米复合材料在光学信息处理中的全光开关领域具有潜在的应用价值。**

关键词: RAFT; N-**苯基马来酰亚胺; 纳米复合物; 光致发光; 非线性光学**

中图分类号: 0437 **文献标识码:** A

0 Introduction

During recent decades, the copolymerization involving N-phenylmaleimide (NPMI) has stimulated great interest, due to the wide possibilities for the preparation of new materials with improved properties such as flame and heat-resistance, thermal and chemical stability [1-7], photosensitivity [8,9] and nonlinear optics(NLO) [10,11]. The synthesis of NPMI copolymers by anionic polymerization [12-15], rare earth coordination catalyst [16] and atom transfer radical polymerization (ATRP) [17-19] have been studied. The reversible addition-fragmentation chain transfer (RAFT) process is a versatile method for control over molecular weight, molecular weight distribution(MWD) , composition and architecture. However, as far as we know, there is few report concerning this [20].

To enhance the thermal stability and PL properties of polymer, the inorganic nanoparticles have been introduced in polymer. The polymer nanocomposites (PNCs) have been studied widely [21-23]. The controllability of PL properties of PNCs need further investigation. The semiconductor quantum dots (QDs) and the PNCs containing QDs also exhibit excellent NLO properties [24-28]. A significant challenge for this kind of nanoparticle is to incorporate them into a matrix while preserving the size distribution and quantum yield. It is well-known that amphipathic polymer exhibit excellent dispersion and surface modification of QDs.

In our present work, the poly(N-phenylmaleimide) (PNPMI) macro-chain transfer agent (MCTA) was synthesized by RAFT polymerization, then the amphipathic poly (N—phenylmaleimide) -b-poly (4-vinylpyridine) -Cd^{2+} (PNPV-Cd^{2+}) complex was synthesized by RAFT polymerization using 4-vinylpyridine-Cd^{2+} (4VP-Cd^{2+}) as the second monomer. The PNPV-CdS nanocomposites were prepared in situ. The CdS content in composites was controlled by the polymerization time. The effects of the CdS content on the structure, photoluminescence (PL) and NLO properties of PNPV-CdS have been discussed for the first time.

1 Experiment

1.1 Materials

The industrial pure NPMI was recrystallized in ethanol. The 4VP was obtained from Aldrich and purified purified under reduced pressure to remove the inhibitor. 4-Vinylpyridine(4VP) (Aldrich) was vacuum distilled prior to polymerization. Thioacetamide(TAA) from Merck was recrystallized in spectroscopic grade benzene and dried at room temperature in a vacuum oven. 4VP-Cd^{2+} was prepared: $Cd(CH_3COO)_2$ was dissolved in 4VP/DMF solution($Cd(CH_3COO)_2$: 4VP = 1∶5 ~ 1∶40, mol∶ mol; 4VP∶ DMF = 1∶2, v∶ v) and stirred at room temperature for 3 days. The chain transfer agents benzyl 9H-carbazole-9-carbodithioate (BCCDT) was synthesized according to the literature [29]. All other reagents and solvents (Aldrich or Fluka) were used as received.

1.2 Preparation of PNPV-CdS nanocomposite

Synthesis of MCTA. MCTA was synthesized by RAFT empolying 2,2′-azobis(isobutyronitrile) (AIBN) as an initiator and BCCDT as a CTA. The polymerization was conducted at 95℃ under a nitrogen atmosphere in septa-sealed vials with the molar ratio NPMI/CTA/AIBN = 300/6/1. The molecular weights (M_n) of polymers were determined by GPC.

Synthesis of PNPV-Cd^{2+}. PNPV-Cd^{2+} was prepared at 80℃ with the molar ratio 4VP-Cd^{2+}/MCTA (M_n = 2413g/mol) /AIBN = 1500/5/1. A DMF solution (100 mL) containing quantitative 4VP-Cd^{2+}, 14 mmol 4VP-Cd^{2+} and 142 mg of AIBN was stirred gently at 80℃ and under N2 over a period of 48 h. The

PNPV-Cd^{2+} obtained was washed by aether/petroleum ether(1:1, v:v) solution. Then the sample was dried in vacuo overnight.

Preparation of PNPV-CdS. PNPV-Cd^{2+} containing quantitative Cd^{2+} ions reacted with TAA(Cd^{2+}: TAA =1:1, mol:mol) in 50mL DMF solution at 65℃ for 1h. The solution was dispersed by ultrasound. The PNPV-CdS nanocomposites obtained were washed by distilled water, dried at room temperature and collected for further characterization.

1.3 Characterization

^{1}H NMR spectra was recorded in DMSO on a Inova-400 instrument using tetra-order methylsilane as a reference. The CdS content in these composites was investigated by means of Inductively Coupled Plasma (ICP) (PLA-SPECI, Leeman company) and Hitachi S-570 scanning electron microscope (SEM) equipped with Energy Dispersive Analysis by X-rays (EDAX) facility. Samples for ICP were prepared by dispersing the product in 98% HNO_3 and then boiling it for 30min. The solution containing Cd was diluted with distilled water. The morphology of the nanoparticles and composites were determined by SEM and Hitachi H-600-II transmission electron microscope (TEM). The Z-average size and the polydispersity index (PDI) of the nanocomposites were measured by Malvern HPP 5001 high performance particle sizer (HPPS) at 25℃. The X-ray diffraction (XRD) patterns were recorded on a Rigaku D/MAX-IIIC X-ray diffractometer using Cu Ka radiation ($\lambda = 0.1542$ nm) operated at 50 kV and 100 mA, with the diffraction angle in the range of the $2\theta = 5 \sim 70°$. Ultraviolet/visible (UV-vis) Absorption Spectroscopy of the samples was recorded on a Shimadzu UV-vis spectrophotometer (UV-2401PC) with the scanning range was from 190 to 700 nm. Absorption from the solvent was subtracted from each spectrum. The photoluminescence (PL) spectra of products were obtained on an Shimadzu Edinburgh-920 spectrophotometer equipped with a 450-W Xe arc lamp and a PMT detector at room temperature. The Z-scan absorption spectroscopy were recorded on a frequency-doubled Nd:YAG laser which produces 7 ns pulses at 532 nm with a repetition rate of 10 Hz.

2 Results and Discussion

2.1 Synthesis and Structural Characterization

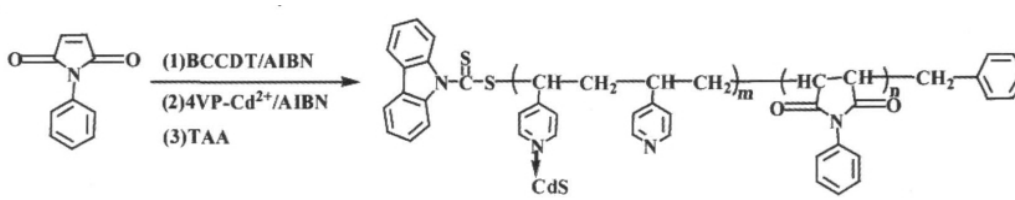

Scheme 1. Schematic chart to form PNPV-CdS nanocomposites

示意图 1 PNPV－CdS 纳米复合物的合成流程示意图

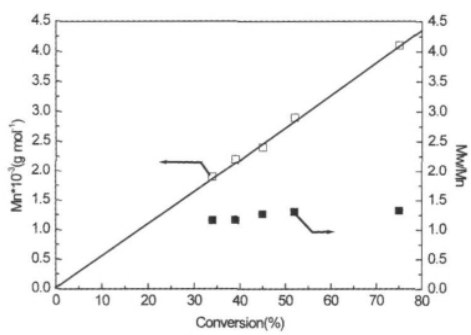

Fig. 1 Effect of conversion on the molecular weight and MWD of PNPMI.

图 1 转化率对 PNPMI 分子量及其分布的影响

The molecular weight and MWD of MCTA increase with the increasing NPMI conversion (Figure 1). The MWD of MCTA is about 1.2 under 40% conversion. With the conversion increases, the MWD of MCTA increases(~1.4). This indicates that the molecular weight and MWD of MCTA can be controlled by RAFT polymerization.

The time－conversion plots for the polymerization of NPMI was shown in Figure 2. Under lower conversion (<40%), the conversion of NPMI increases with the increasing polymerization time, indicates its living na-

ture.

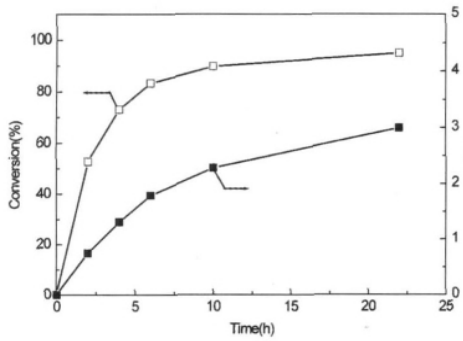

Fig 2　Time-conversion and first-order kinetic plots for the polymerization of NPMI.

图 2　NPMI 聚合的时间 - 转化率和一阶动力学曲线图

The PNPV - Cd^{2+} was synthesized by RAFT using AIBN as initator, 4VP - Cd^{2+} as monomer and PNPMI (M_n = 2413g/mol) as MCTA. The polymerization was performed at 95℃ with a material ratio of [4VP - Cd^{2+}] / [MCTA] / [AIBN] = 1600/40/1.

The ^1H NMR spectra ($CDCl_3$/TMS) of BCCDT, MCTA and PNPV - Cd^{2+} are shown in Figure 3. The marked peaks of PNPV - Cd^{2+} locate δ8.00 - 8.42, δ7.30 - 7.40, δ6.38 - 6.39, δ2.87 - 2.94, δ3.75 and δ1.73ppm, respectively.

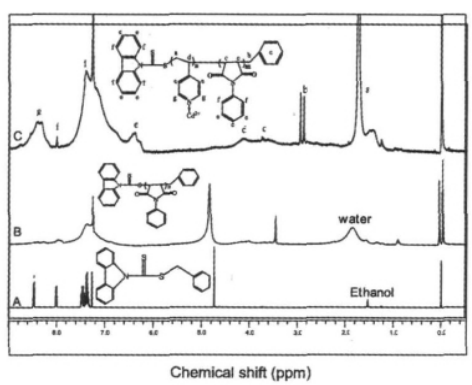

Fig. 3　^1H NMR spectra of BCCDT, MCTA and PNPV - Cd^{2+}

图 3　BCCDT, MCTA 和 PNPV - Cd^{2+} 的 ^1H NMR 谱图

As shown in Figure 4, the conversion of 4VP-Cd^{2+} increases with the increasing polymerization time, indicating its living nature. The M_n of PNPV-Cd^{2+} can be caculated by ^1H NMR: $M_n = 2413 + 2 \times 219.6 \times I_{8.4}/I_{8.0}$, where 2413 is the M_n of MCTA, 219.6is the M_n of 4VP - Cd^{2+}, $I_{8.4}$ and $I_{8.0}$ are the integral value of δ8.4(4VP - Cd^{2+}) and δ8.0(carbazole) .

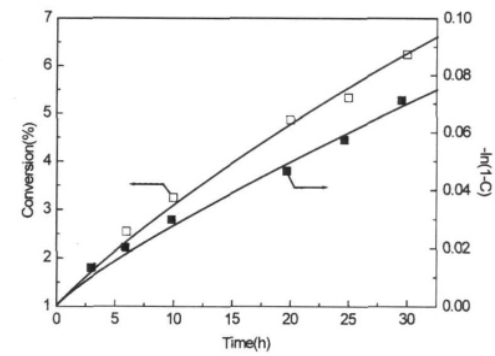

Fig. 4　Time-conversion and first-order kinetic plots for the polymerization of PNPV-Cd^{2+}

图 4　PNPV-Cd^{2+} 的时间-转化率和一阶动力学曲线

The effect of polymerization time on the CdS content in the PNPV-CdS is shown in Table 1. The CdS content increases from PNPV-CdS-0.8 to PNPV-CdS-3.4 with prolonging the block polymerization time from 3h to 28h. This indicates that the CdS content in the PNPV-CdS can be controlled by RAFT polymerization.

The copolymerizayion of NPMI and 4VP-Cd^{2+} and the formation of CdS also can be characterized by FT-IR。As shown in Figure 5, the characteristic vibration of CdS locate 563 cm^{-1} in curve (a) , curve (b) and curve (c) , indicating the formation of CdS. The characteristic vibration of imide in the PNPV-Cd^{2+} and PNPV-CdS locate 1072 and 995 cm^{-1}. The vibration of pyridine in the PNPV-CdS (~1450 cm^{-1}) shows a 8 cm^{-1} blue shift compared with that of PNPV-Cd^{2+} (1458) , indicating the strong interaction between nano CdS and 4VP group [30]. Similarly, the strong interaction between nano CdS and 4VP group in PNPV-CdS also is observed.

表 1　聚合时间对 CdS 含量的影响

Table. 1　Dependence of CdS content on the polymerization time

Label	PNPV-CdS-0.8	PNPV-CdS-1.2	PNPV-CdS-1.8	PNPV-CdS-2.3	PNPV-CdS-2.6	PNPV-CdS-3.4
Polymerization Time(h)	3	6	10	20	24	28
CdS content(wt%)	0.8	1.2	1.8	2.3	2.6	3.4

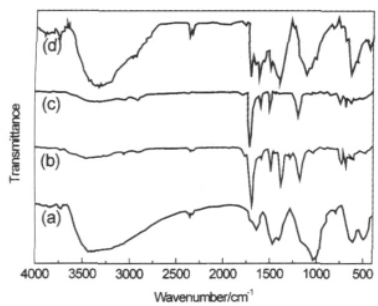

Fig. 5 FTIR spectra of samples: (a) CdS; (b) PNPMI; (c) PNPVP-Cd^{2+} and (d) PNPVP-CdS-3.4

图 5 (a) CdS; (b) PNPMI; (c) PNPVP-Cd^{2+} **和** (d) PNPVP-CdS-3.4 **的** FTIR **谱图**

2.2 Dependence of Morphology of PNPV-Cd^{2+} on the Polymerization Time

The P4VP-Cd^{2+} block length in PNPV-Cd^{2+} increases as the polymerization time prolonging. Thus, the interaction between polymer chains increases. As shown in Figure 6, the PNPV-Cd^{2+} tend to congregate as the polymer chains increases, combining with shrink of particle size from ~200nm to ~100 ~ 120nm. The tunable morphology of hydrogen-bonding interpolymer complexes is assigned to the increasing interaction between polymer chains [31-34].

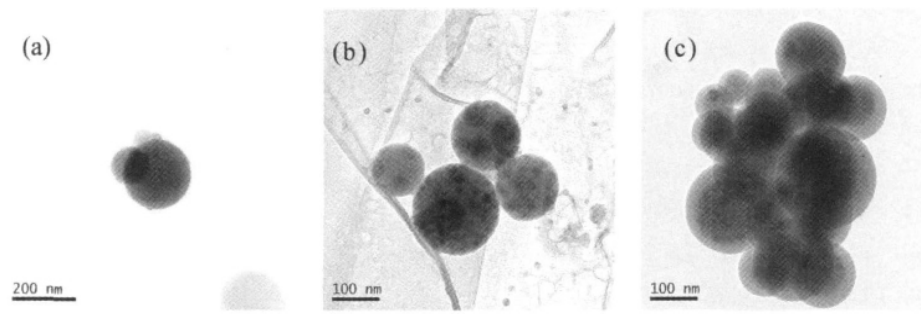

Fig. 6 Tunable TEM morphology of PNPV-Cd^{2+} with different polymerization time: (a) 3h; (b) 10h and (c) 28h.

图 6 聚合时间对 PNPV-Cd^{2+} TEM **形貌的影响:** (a) 3h; (b) 10h **和** (c) 28h.

2.3 Dependence of Morphology of PNPMI-b-P4VP-CdS and CdS Structure on the CdS Content

XRD patterns of PNPV-Cd^{2+}, PNPV-CdS-0.8, PNC-1.2 and CdS are shown in Figure 7. The diffraction peaks at $2\theta = 19.06°$ (Figure 7a ~ 7c) corresponds to amorphous PNPMI-b-P4VP. The XRD patterns of PNPV-CdS-0.8, PNPV-CdS-1.2 and CdS indicate both the cubic and hexagonal CdS crystal structure for the nanoparticles. The hexagonal phase of CdS is gradually instead of the mixed phase of cubic and hexagonal with the CdS content increasing. The crystallinity transformation may be driven by the Cd-to-S ratio.

The average diameter of CdS particles was estimated according to the Debby-Scherer's equation: $L_{hkl} = k\lambda/(B\cos\theta)$, where k is taken as 1, $\lambda = 0.15418$ nm and B(radian) is the half width of the diffraction peak [35,36]. The size of CdS increases from ~1.3nm (Figure 7a) to 7 nm (Figure 7c). This indicates that the CdS nanoparticles congregate together as the CdS content increases.

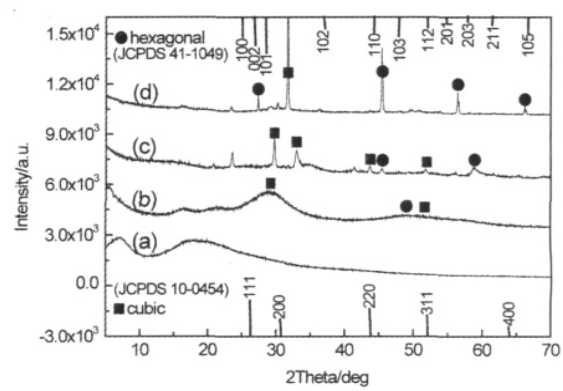

Fig. 7 XRD patterns of (a) PNPV-Cd^{2+}; (b) PNPV-CdS-0.8; (c) PNPV-CdS-1.2; (d) PNPV-CdS-3.4 and the standard cubic (JCPDS 10-0454) and hexagonal (JCPDS 41-1049) CdS XRD patterns.

图 7 XRD **谱图:** (a) PNPV-Cd^{2+}; (b) PNPV-CdS-0.8; (c) PNPV-CdS-1.2; (d) PNPV-CdS-3.4 **和立方** (JCPDS 10-0454)、**六方** (JCPDS41-1049) CdS **的标准谱图**

The structure of nanocomposites was also studied by TEM measurement (Figure 8). The average size of the CdS nanocrystals is about 3 ~ 4 nm in PNPV-CdS-0.8, which is larger than that calculated from XRD

(~1.3 nm). The difference may be due to aggregation of the CdS nano-crystals. The data calculated from XRD results reflected the size of a single crystal, while the TEM photograph shows the aggregates of the CdS particles. As the CdS content increases, as shown in Figure 8(b)~8(d), the CdS particles are about ~5~10 nm. This indicates that the morphology of the PNPV-CdS and the size of CdS nanoparticle can be controlled by adjusting the content of CdS through RAFT polymerization.

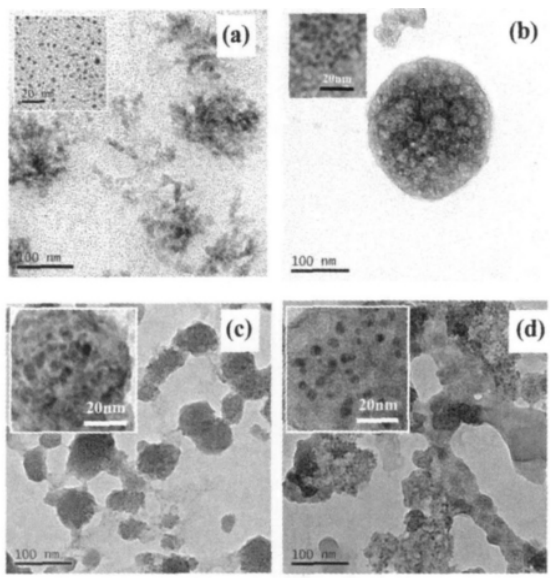

Fig. 8　TEM morphology of (a) PNPV-CdS-0.8; (b) PNPV-CdS-1.8; (c) PNPV-CdS-2.3 and (d) PNPV-CdS-3.4.

图 8　TEM 图像: (a) PNPV-CdS-0.8; (b) PNPV-CdS-1.8; (c) PNPV-CdS-2.3 **和** (d) PNPV-CdS-3.4.

The dispersion of PNPV-CdS also determined by HPPS. As shown in Figure 9, the size of PNPV-CdS increases from ~120nm to ~200nm with CdS content increasing from 0.8 wt% to 3.4 wt%, due to the conglomeration of PNPV-CdS. This is consistent with TEM results.

2.4　Dependence of Absorption and PL properties of PNPMI-b-P4VP-CdS on the CdS Content

The absorption spectra of PNPV-Cd^{2+} prepared with different polymerization time and the PNPV-CdS containing different CdS content are shown in Figure 10. As the polymerization time increases from 3h to 28h, the absorption intensity of PNPV-Cd^{2+} increases, due to the increasing block length of P4VP-Cd^{2+}. A slight red shift from curve a to curve d also is observed. The intensity of absorption spectra of PNPV-CdS also increases from PNPV-CdS-0.8 to PNPV-CdS-3.4 with the increasing CdS content. By comparison, the marked absorption peaks of PNPV-CdS show a larger red shift (from 269 nm to 308 nm) than that of PNPV-Cd^{2+} (from 268 nm to 270 nm), indicating that the CdS nanoparticles congregate together as the CdS content increase. This is assigned to the surface effect of nano CdS, combining with the hydrogen bond interaction between P4VP block.

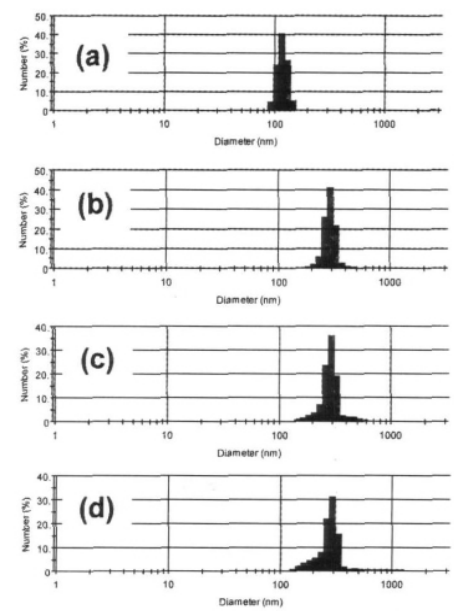

Fig. 9　The dispersion of PNPMI-b-P4VP-CdS by HPPS: (a) PNPV-CdS-0.8; (b) PNPV-CdS-1.8; (c) PNPV-CdS-2.3 and (d) PNPV-CdS-3.4.

图 9　PNPMI-b-P4VP-CdS 的分散性(HPPS 检测) (a) PNPV-CdS-0.8; (b) PNPV-CdS-1.8; (c) PNPV-CdS-2.3 **和** (d) PNPV-CdS-3.4.

The PL spectra of samples are shown in Figure 11. The characteristic peaks of PNPV-Cd^{2+} locate 344~361 nm. The PL intensity of PNPV-Cd^{2+} increases with the increasing polymerization time from 3h to 28h, resulting from the increase of P4VP-Cd^{2+} block length. By comparison, the marked peaks of PNPV-CdS locate 344~361 nm and 438 nm, corresponding to PNPMI-b-P4VP and CdS, respectively. The PL intensity of PNPMI-b-P4VP decreases with the incrasing CdS con-

tent, from PNPV-CdS-0.8 to PNPV-CdS-3.4. However, the PL intensity of CdS increases as the CdS content increases, indicating the PNPMI-b-P4VP-to-CdS charge transfer.

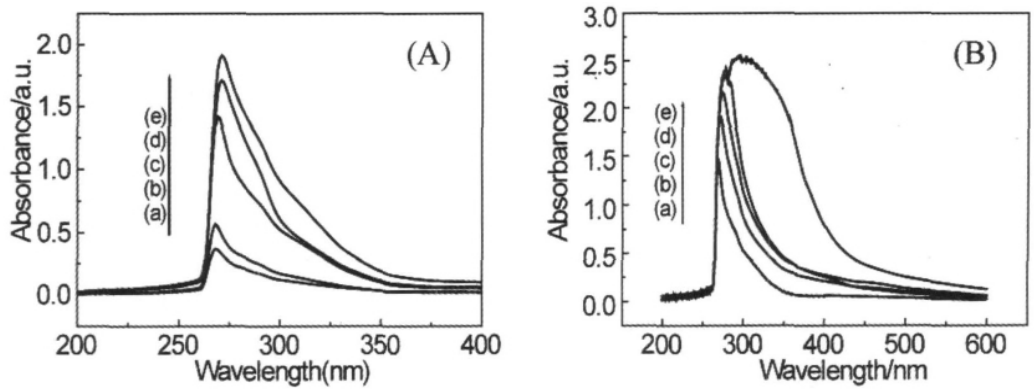

Fig. 10 Absorption spectra of samples: (A) PNPMI-b-P4VP-Cd^{2+} with different polymerization time: (a) 3h; (b) 10h; (c) 20h; (d) 24h and (d) 28h ($\lambda ex = 293nm$, 0.2g/L DMF solution); (B) PNPV-CdS with different CdS content: (a) PNPV-CdS-0.8; (b) PNPV-CDS-1.8; (c) PNPV-CdS-2.3; (d) PNPV-CdS-2.6 and (e) PNPV-CdS-3.4 ($\lambda ex = 294nm$, 0.2g/L DMF solution).

图 10 样品的吸收光谱: (A) **不同聚合时间的** PNPMI-b-P4VP-Cd^{2+}: (a) 3h; (b) 10h; (c) 20h; (d) 24h **和** (d) 28h ($\lambda ex = 293nm$, 0.2g/L DMF **溶液**); (B) **不同** CdS **含量的** PNPV-CdS: (a) PNPV-CdS-0.8; (b) PNPV-CDS-1.8; (c) PNPV-CdS-2.3; (d) PNPV-CdS-2.6 **和** (e) PNPV-CdS-3.4 ($\lambda ex = 294nm$, 0.2g/L DMF **溶液**).

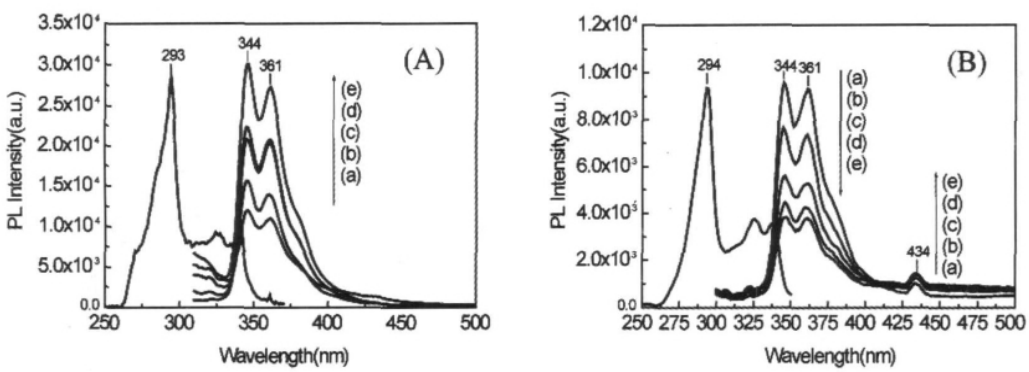

Fig. 11 PL spectra of samples: (A) PNPV-Cd^{2+} with different polymerization time: (a) 3h; (b) 10h; (c) 20h; (d) 24h and (d) 28h ($\lambda ex = 293nm$, 0.2g/L DMF solution); (B) PNPV-CdS with different CdS content: (a) PNPV-CdS-0.8; (b) PNPV-CdS-1.8; (c) PNPV-CdS-2.3; (d) PNPV-CdS-2.6 and (e) PNPV-CdS-3.4 ($\lambda ex = 294nm$, 0.2g/L DMF solution).

图 11 PL 光谱: (A) **不同聚合时间的** PNPV-Cd^{2+}: (a) 3h; (b) 10h; (c) 20h; (d) 24h **和** (d) 28h ($\lambda ex = 293nm$, 0.2g/L DMF **溶液**); (B) **不同** CdS **含量的** PNPV-CdS: (a) PNPV-CdS-0.8; (b) PNPV-CdS-1.8; (c) PNPV-CdS-2.3; (d) PNPV-CdS-2.6 **和** (e) PNPV-CdS-3.4 ($\lambda_{ex} = 294nm$, 0.2g/L DMF **溶液**).

The PL spectra of PNPV-Cd^{2+} and PNPV-CdS powders also were obtained. The marked excitation and emission peaks of samples are shown in Figure 12. The peaks at 363/439 nm, 372/438 nm and 553/620 nm belong to PNPV-Cd^{2+}, PNPV-CdS-0.8 and PNPV-CdS-3.4, respectively. The PNPV-CdS shows a red shift compared with that of PNPV-Cd^{2+}, due to the formation of CdS. The excitation and emission peaks of PNPV-CdS-3.4 exhibit 181nm and 182 nm red shifts compared with that of PNPV-CdS-0.8. This indicates that the CdS congregated particles bring about the non-radiative energy transfer (NRET) between PNPMI-b-P4VP and CdS nanoparticles. This also indicates that the PL of PNPV-CdS can be controlled by RAFT method.

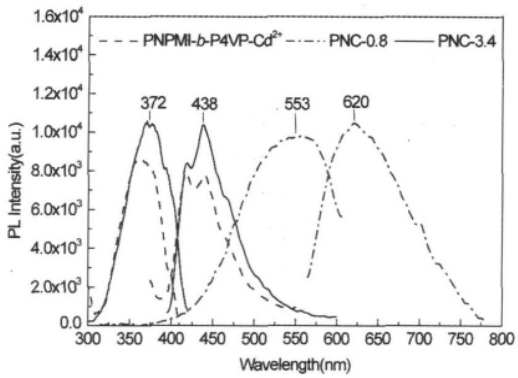

Fig. 12　PL spectra of PNPV-Cd^{2+} (λ_{ex} = 363nm) , PNPV-CdS-0. 8(λ_{ex} = 372nm) and PNPV-CdS-3. 4(λ_{ex} = 553nm) powders.

图 12　粉末荧光谱图: PNPV-Cd^{2+} (λ_{ex} = 363nm) , PNPV-CdS-0. 8(λ_{ex} = 372nm) **和** PNPV-CdS-3. 4(λ_{ex} = 553nm)

2. 5　Effect of CdS on the NLO properties of PNPV-CdS

To determine the effect of CdS on the NLO properties of PNPV-CdS, the samples were scanned with the open aperture (S = 1) and closed aperture (S = 0. 31) . Figure 13 shows the Z-scan measurement data with the open aperture(Figure 13A) and closed aperture (Figure 13B) , which contain both contributions from the nonlinear absorption and nonlinear refractive index.

As shown in Figure 13A, the nonlinear absorption intensity of samples go as PNPV-Cd^{2+} < CdS < PNPV-CdS-0. 8 < PNPV-CdS-1. 8, which is consistent with order of the nonlinear refractive intensity of samples. According to Z-scan theory [37] , the nonlinear refractive index n2 is related to ΔT_{p-v} as: $n_2 = \lambda\alpha / [0.812\pi I_0 (1-\exp(-\alpha L))] \times \Delta T_{p-v}$, Where ΔT_{p-v} is the difference between the normalized peak and valley transmittances of the apertured Z-scan, I_0 is the pulse irradiance, λ is the laser wavelength(532nm) , α is the linear absorption coefficient, L is the sample thickness(2 mm) . While the third-order susceptibility $\chi^{(3)}$ (in m^2/V^2) is linked to n_2 through $\chi^{(3)} = 4/3\varepsilon_0 c n_0^2 \times n_2$, Where c is the light speed in vacuum, ω is the optical pulsation, and n_0 is the linear refractive index of the medium, which we approximate here to the n_0 (= 1. 424 for DMF) value of the solvent.

According to these equations, we obtained the third-order NLO polarizability ($\chi^{(3)}$) of 4.34×10^{-12} esu, 6.14×10^{-12} esu and 4.5×10^{-11} esu for CdS, PNPV-CdS-0. 8 and PNPV-CdS-1. 8, respectively. However, the third-order NLO response of P PNPV-Cd^{2+} is not observed. By comparison between PNPV-CdS-0. 8 and PNPV-CdS-1. 8 we can see that the nonlinear optical response is enhanced by CdS combining with the increase of CdS content. The surface-induced large separation of charge between the delocalized electron and localized hole is the origin of the large nonlinear optical response of PNPV-CdS. The surface-induced charge separation i. e. the coherent oscillation of the conduction band electrons is expected to enhance the anisotropic polarization and hence the nonlinear optical response [38,39] .

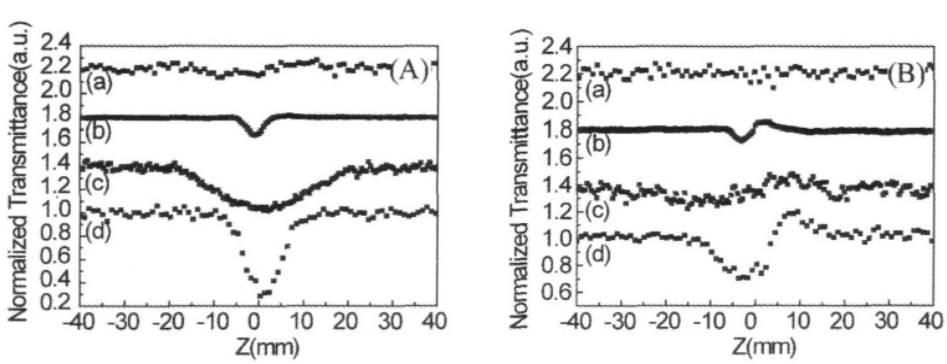

Fig. 13　Z-scan with the input irradiance of 28. 8μJ. The normalized energy transmissions of Z-scan experiments with open aperture (S = 1, A) and closed aperture(S = 0. 31, B) for (a) PNPV-Cd^{2+}; (b) CdS; (c) PNPV-CdS-0. 8 and (d) PNPV-CdS-1. 8, respectively. The NLO properties of the samples were investigated with 532 nm laser pulses of 4. 6 ns duration using Nd: YAG laser.

图 13　532 nm, 4. 6 ns 脉冲宽度的 Nd: YAG **激光脉冲 (28. 8μJ) 激发的** PNPV-Cd^{2+} **归一化开孔(** S = 1, A) **、闭孔(** S = 0. 31, B) **Z-扫描谱图:** (a) PNPV-Cd^{2+}; (b) CdS; (c) PNPV-CdS-0. 8 and (d) PNPV-CdS-1. 8.

3 Conclusion

This work demonstrates RAFT synthesis of amphipathic PNPV-Cd^{2+} and in-situ preparation of PNPV-CdS. The content and size of CdS in nanocomposites were controlled by the polymerization time. As a result, the PL properties of the PNPV-CdS nanocomposites also were tunable. The third-order nonlinear optical properties of PNPV-CdS is stronger than that of CdS and PNPMI-*b*-P4VP, this is assigned to the strong interaction between CdS and PNPMI-*b*-P4VP. This nanocomposite improves the film-forming ability due to the introduction of flexible polymer and has potential applications in optical limiting device.

Acknowledgements

Authors gratefully thank the Chinese Natural Science Foundation No. 20876101 and No. 21071105, and major project of college and 30 universities Jiangsu Province (08KJA430004).

References

[1] Serap Senel, Zakir M. O. Rzaev, Erhan Pi kin. Copolymerization of N-phenylmaleimide with 2-hydroxyethyl and ethyl methacrylates [J]. Polymer International, 2003, 52: 713 - 721.

[2] Shouji Iwatsuki, Masataka Kubo, Makoto Wakita, Yasue Matsui, Hideki Kanoh. Polymerization thermodynamics N - phenylmaleimide and copolymerization with styrene and phenyl vinyl sulfide [J]. Macromolecules, 1991, 24: 5009 - 5014.

[3] Luminita Cianga, Ayfer Sarac, Koichi Ito, Yusuf Yagci. Synthesis and characterization of new alternating, amphiphilic, comblike copolymers of poly(ethylene oxide) macromonomer and N - phenylmaleimide [J]. Journal of Polymer Science Part A: Polymer Chemistry, 2005, 43: 479 - 492.

[4] Akikazu Matsumoto, Takeshi Kimura. Synthesis of heat - and solvent - resistant polymers by radical polymerization of trifluoromethyl - substituted N - phenylmaleimides [J]. Journal of Applied Polymer Science, 1998, 68: 1703 - 1708.

[5] Jayant S. Parmar, Chetan G. Patel, Dinesh K. Patel. Functional poly(N - phenylmaleimide) as a cation exchanger - II [J]. High Performance Polymers. 1991, 3(2): 89 - 98.

[6] Guadalupe del C. Pizarro, Oscar G. Marambio, Manuel Jeria Orell, Margarita Huerta, Bernabé L. Rivas. Synthesis, characterization, and metal complexation of poly(N - phenylmaleimide - co - acrylic acid) and poly(N - phenylmaleimide - co - acrylamide) as polychelatogens in aqueous solution [J]. Journal of Applied Polymer Science, 2006, 99: 2359 - 2366.

[7] Yue - Xin Wang, Jing - Wei Long, Liu - Cheng Zhang. Preparation and Characterization of St - Npmi Copolymer/Montmorillonite Nanocomposites [J]. Polymer Materials Science and Engineering, 2004, 20(5): 197 - 199.

[8] Hongyu Jun, Xuesong Jie. Novel chemical - bonded polymerizable sulfur - containing photoinitiators comprising the structure of planar N - phenylmaleimide and benzophenone for photopolymerization [J]. Polymer, 2006, 47: 4967 - 4975.

[9] Jun Young, Tae Ho. Synthesis of N - (phenyl) maleimide - based photopolymer and its application to photo - aligning of LC molecules [J]. Reactive functional polymers, 2002, 53: 83 - 89.

[10] Ki Hong, Jong Tae, Sangyup S. Mi Gyung, Chul Joo, Nakjoong K. Synthesis and properties of novel crosslinkable second - order nonlinear optical polymers based on 2,3,4,5,6 - pentafluorostyrene [J]. Reactive functional polymers, 1999, 40: 169 - 175.

[11] Ji Yong, Tae Ja, Man Jung, Dong Hoon, Nakioong. N - phenylmaleimide polymers for second - order nonlinear optics [J]. Polymer, 1997, 38(18): 4651 - 4656.

[12] Shin - ichi Fumio, Takeshi E. Spontaneous Alternating Copolymerization of Methoxyallene with N - Phenylmaleimide [J]. Macromolecules, 1999, 32: 5501 - 5506.

[13] Seema Mathias, Friederike T. Synthesis, characterization and properties evaluation of copolymers of 2,3,4,5,6 - pentafluorostyrene and N - phenylmaleimide [J]. Polymer International, 2005, 54: 1620 - 1625.

[14] Xiujuan Xi, Liming Jiang, Weilin Sun, Zhiquan Shen. Synthesis and anionic polymerization of optically active N - phenylmaleimides bearing bulky oxazoline substituents [J]. European Polymer Journal. 2005, 41: 2592 - 2601.

[15] Tokio Hagiwara, Takamasa Shimizu, Tsutomu Someno, Takashi Yamagishi, Hiroshi Hamana, Tadashi Narita. Anionic polymerization of N - substituted maleimide. 4. "Living" characteristics of anionic polymerization of N -

phenylmaleimide [J]. Macromolecules, 1988, 21: 3324 - 3327.

[16] Yanbing Lu, Weilin Sun, Zhiquan Shen. Copolymerization of N - phenylmaleimide with styrene by rare earth coordination catalyst [J]. European Polymer Journal, 2002, 38: 1275 - 1279.

[17] Ren Qiang, Jiang Bibiao, Zhang Dongliang, Yu Qiang, Fang Jianbo, Yang Yang, Chen Jianhai. Studies on the atom transfer radical polymerization of a maleimide AB* monomer and modification of the halogen end groups [J]. European Polymer Journal, 2005, 41: 2742 - 2752.

[18] Y. Yuan, A. Siegmann, M. Narkis, J. P. Bell. Emulsion copolymerization of N - phenylmaleimide with styrene [J]. Journal of Applied Polymer Science. 1996, 61: 1049 - 1054.

[19] Shuichi Kanno, Masayoshi Hosoi, Tateaki Ogata, Makoto Takeishi. Polymerization of N - Phenylmaleimide initiated by 9 - borabicyclo [3. 3. 1] nonane [J]. Polymer International, 1997, 42: 321 - 327.

[20] Graeme Moad, Ezio Rizzardo, San H. Thang. Radical additione fragmentation chemistry in polymer synthesis [J]. Polymer, 2008 49: 1079 - 1131.

[21] WANG Yue - xin, LONG Jing - wei, ZHANG Liu - cheng. Preparation and characterization of St - NPMI copolymer/montmorillonite nanocomposites [J]. Polymeric Materials Science & Engineering, 2004, 20: 197 - 199.

[22] P. K. Khanna, Sunil. P. Lonkar, V. V. V. S. Subbarao, Ki - Won Jun. Polyaniline - CdS nanocomposite from organometallic cadmium precursor [J]. Materials Chemistry and Physics, 2004, 87: 49 - 52.

[23] Yanmao Dong, Jianmei Lu, Qingfeng Xu. Fluorescence Studies on Thiol - Functional Polystyrene - CdS Nanocomposites [J]. Journal of Macromolecular Science, Part A. 2008, 45: 37 - 43.

[24] Bing Liu, Heping Li, Chwee Har Chew, Wenxiu Que, Yee Loy Lam, Chan Hin Kam, Leong Ming Gan, Guo Qin Xu. PbS - polymer nanocomposite with third - order nonlinear optical response in femtosecond regime [J]. Materials Letter, 2001, 51: 461.

[25] Dabin Yu, Xiaoquan Sun, Jintian Bian, Zhongcheng Tong, Yitai Qian. Gamma - radiation synthesis, characterization and nonlinear optical properties of highly stable colloidal silver nanoparticles in suspensions [J]. Physica E, 2004, 23: 50 - 55.

[26] Xiaohui Wang, Yumin Du, Sha Ding, Ququan Wang, Guiguang Xiong, Min Xie, Xincheng Shen, Daiwen Pang. Preparation and Third - Order Optical Nonlinearity of Self - Assembled Chitosan/CdSe - ZnS Core - Shell Quantum Dots Multilayer Films [J]. The Journal of Physical Chemistry B, 2006, 110: 1566 - 1570.

[27] Yu Zhang, Ming Ma, Xin Wang, Degang Fu, Haiqian Zhang, Ning Gu, Juzheng Liu, Zuhong Lu, Ling Xu, Kunji Chen. Second - order optical nonlinearity of surface - capped CdS nanoparticles and effect of surface modification [J]. Journal of Physics and Chemistry of Solids, 2003, 64: 927 - 931.

[28] H. Du, G. Q. Xu, and W. S. Chin, L. Huang, W. Ji. Synthesis, Characterization, and Nonlinear Optical Properties of Hybridized CdS - Polystyrene Nanocomposites [J]. Chemistry of Materirals, 2002, 14: 4473 - 4479.

[29] Di Zhou, Xiulin Zhu, Jian Zhu, Haishu Yin. Influence of the chemical structure of dithiocarbamates with different R groups on the reversible addition - fragmentation chain transfer polymerization [J]. Journal of Polymer Science Part A: Polymer Chemistry, 2004, 205: 1125 - 1128.

[30] K. H. Wu, Y. R. Wang, W. H. Hwu. FTIR and TGA studies of poly(4 - vinylpyridine - co - divinylbenzene) - Cu(II) complex [J]. Polymer Degradation and Stability, 2003, 79: 195 - 200.

[31] Maria Sotiropoulou, Julian Oberdisse, Georgios Staikos. Soluble hydrogen - bonding interpolymer complexes in water: A small - angle neutron scattering study [J]. Macromolecules. 2006, 39: 3065 - 3070.

[32] M. Sotiropouloua, C. Cincub, G. Bokiasc, G. Staikos. Water - soluble polyelectrolyte complexes formed by poly (diallyldimethylammonium chloride) and poly(sodium acrylate - co - sodium 2 - acrylamido - 2 - methyl - 1 - propanesulphonate) - graft - poly(N, N - dimethylacrylamide) copolymers [J]. Polymer, 2004, 45: 1563 - 1568.

[33] Evaggelia Serefoglou, Julian Oberdisse, Georgios Staikos. Characterization of the soluble nanoparticles formed through coulombic interaction of bovine serum albumin with anionic graft copolymers at low pH [J]. Biomacromolecules, 2007, 8: 1195 - 1199.

[34] Maria Sotiropoulou, Frederic Bossard, Eric Balnois, Julian Oberdisse, Georgios Staikos. Characterization of the core - shell nanoparticles formed as soluble hydrogen - bonding interpolymer complexes at low pH [J]. Langmuir, 2007, 23: 11252 - 11258.

[35] Suhua Wang, Shihe Yang, Chunlei Yang, Zongquan Li, Jiannong Wang, Weikun Ge, W. Poly(N - vinylcarbazole) (PVK) Photoconductivity Enhancement Induced by

Doping with CdS Nanocrystals through Chemical Hybridization [J]. The Journal of Physical Chemistry B, 2000, 104: 11853 – 11858.

[36] Weijun Liu, , Weidong He, Zhicheng Zhang, Cheng Zheng, Jian Li, Hao Jiang, Xuewu Ge , Huarong Liu. Fabrication of CdS nanorods in inverse microemulsion using HEC as a template by a convenient γ – irradiation technique [J]. Journal of Crystal Growth, 2006, 290: 592 – 596.

[37] W. Ji, Hendry Izaac Elim, Jun He, F. Fitrilawati, C. Baskar, S. Valiyaveettil, W. Knoll . Photophysical and Nonlinear – Optical Properties of a New Polymer: Hydroxylated Pyridyl Para – phenylene [J]. The Journal of Physical Chemistry B, 2003, 107: 11043 – 11047.

[38] Bing Liu, Heping Li, Chwee Har Chew, Wenxiu Que, Yee Loy Lam, Chan Hin Kam, Leong Ming Gan, Guo Qin Xu. PbS – polymer nanocomposite with third – order nonlinear optical response in femtosecond regime [J]. Materials Letters, 2001, 51: 461 – 469.

[39] Dabin Yu, Xiaoquan Sun, Jintian Bian, Zhongcheng Tong, Yitai Qian. Gamma – radiation synthesis, characterization and nonlinear optical properties of highly stable colloidal silver nanoparticles in suspensions [J]. Physica E: Low – dimensional Systems and Nanostructures, 2004, 23: 50 – 55.